第32卷第3期
2013年6月

红外与毫米波学报
J. Infrared Millim. Waves

Vol. 32, No. 3
June, 2013

文章编号:1001-9014(2013)03-0198-07

DOI:10.3724/SP.J.1010.2013.00198

Signature analysis and 3-D reconstruction of rectangular building in very high resolution SAR images

TANG Kan, FU Kun, SUN Xian, SUN Hao, WANG Hong-Qi

(The Key Laboratory of Technology in Geo-spatial Information Processing and Application System, Institute of Electronics, Chinese Academy of Sciences, Beijing 100190, China)

Abstract: The new advanced very high resolution (VHR) synthetic aperture radar (SAR) sensors are capable of achieving sub-metric spatial resolution, which offers the opportunity for a fine level of analysis of man-made structures in such data. In this paper, we first proposed a decomposed model to analyze the signature of rectangular buildings in VHR SAR images. In the model, the scattering effects were subdivided according to different contributors. Accordingly, detailed geometrical structures and spatial distributions of image features of building objects with respect to varied SAR illumination conditions were exploited. Then, based on the generalized effects, a new detection and reconstruction algorithm was proposed for 3-D reconstruction from single VHR SAR images. Specifically, a matching procedure was applied to extract image features, and prior knowledge was employed in the reconstruction steps to jointly perform dimensions retrieval and building type identification. Finally, the proposed approach was applied to VHR SAR imagery and the reconstruction results were discussed.

Key words: rectangular building reconstruction; VHR SAR image; non-orthogonal aspect angle

PACS: 89.20.Kk

高分辨率SAR图像中矩形建筑物特性分析与三维重建

唐 侃, 付 锟, 孙 显, 孙 皓, 王宏琦

(中国科学院电子学研究所 中国科学院空间信息处理与应用系统技术重点实验室,北京 100190)

摘要:近年来不断发展成熟的合成孔径雷达技术将获取的图像分辨率提高到分米级.在高分辨率条件下,建筑物在SAR图像上表现出的空间信息更加丰富,结构特征更加明显.首先提出了分解模型对高分辨SAR图像中矩形建筑物的特性进行详细分析.在此模型中,散射效应根据不同的贡献来源被细分,以便于解析建筑物图像特征在不同的SAR成像条件下的几何结构和空间分布规律.然后基于建筑物图像表征的结构先验,提出了一种新的单幅高分辨率SAR图像建筑物检测和3-D重建算法,其中包括模型匹配的图像特征的提取,以及先验引导的重建过程.最后,选用了实际高分辨率SAR图像进行建筑物检测和三维重建实验并对重建结果进行了讨论.

关 键 词:矩形建筑物重建;高分辨率SAR图像;多姿态角

中图分类号:TN959.73 **文献标识码**:A

Introduction

The 3-D building reconstruction is one of the key issues for information retrieval from SAR images. Typical characteristics of buildings, like layover, shadow and double-bounce effects are analyzed and utilized mostly for detection or geometric dimension retrieval. However, 3-D reconstruction by direct feature measurement from single aspect SAR images usually gives limited results due to the poor performance of primitive object detection and identification. Techniques incorporating complimentary data from, e.g. interferometric

Received date: 2012-09-03, **revised date**: 2012-09-28 **收稿日期**:2012-09-03, **修回日期**:2012-09-28

Foundation items: Supported by the National Natural Science Foundation of China (41001285) and Major projects of High-resolution observation to Earth (E0303/1112)

Biography: TANG Kan(1984-), female, Beijing, China, Doctor. Research field is SAR image processing and target recognition. E-mail: tangkan08@mails.ucas.ac.cn

techniques, multi-aspects images or optical imagery for feature extraction have achieved accuracy improvement[1-3], but their applications are limited by the availability of proper data. Other approaches, based on geometric or electromagnetic models, have been developed for building reconstruction[4-5]. These approaches are capable of extracting height parameter from single SAR image with high accuracy through either a deterministic approach which inverts electromagnetic models to solve the height parameter[4], or a hypothesis-match procedure which iteratively matches the simulation or projection of building hypothesis with real data to optimize height parameter[5]. However, more prior parameters are required. So, 3-D reconstruction from single aspect SAR image is still a challenge that more supplementary information of building in SAR image are needed. Fortunately, on the VHR SAR data provided by modern airborne sensors, additional features of buildings like edges, roof patches become discernable even in layover area[6], which offers the possibility for a fine level of signature analysis.

In this paper, we focus on analyzing the signature of rectangular buildings with either flat or gable roof in VHR SAR images to effectively support 3-D reconstruction from single VHR SAR data. The novel contributions are as follows: First, a decomposed model which subdividing the building scatterings into different terms according to their geometrical contributors is proposed for magnitude image analysis. The model not only gives a set of comprehensive expressions which link the building dimensions to image features without ambiguity, but also facilitates the structural analysis of each feature and the configuration of building area under varied SAR illumination conditions. Second, a new detection and reconstruction algorithm utilizing the revealed effects is proposed to perform the 3-D reconstruction from single VHR SAR image. In the algorithm, a match-based method is applied to extract image features by importing the feature shape prior, meanwhile the reconstruction process is jointly performed for dimension retrieval and building type identification based on the distribution information of the building area. We demonstrate the applicability of the approach through the 3-D building reconstruction from single VHR SAR data and the results valid the proposed method.

1　A decomposed model for the analysis of building signature in VHR SAR images

In our paper, the decomposed model further subdivides the main scattering effects according to their geometric contributors, in our case, the roof and wall.

1.1　Decomposing building features in the range direction

Fig. 1 (a1) and Fig. 2 (a1) show examples of the slant range profiles of two rectangular buildings with different roof types viewed by a SAR sensor at incidence angle θ. w_r, w_r^F and w_r^B are the irradiated width of the whole roof, the size of the sensor near roof patch and sensor far roof patch at this range profile respectively. , denote the wall height and roof height. In the decomposed model, as shown in Figs. 1 (b1), (c1) and Figs. 2 (b1), (c1), the returned signal is decomposed into roof scattering and wall scattering and the occlusion areas are subdivided into roof shadow and wall shadow. The expressions linking the image parameters to building dimensions in the range direction are generalized as follows:

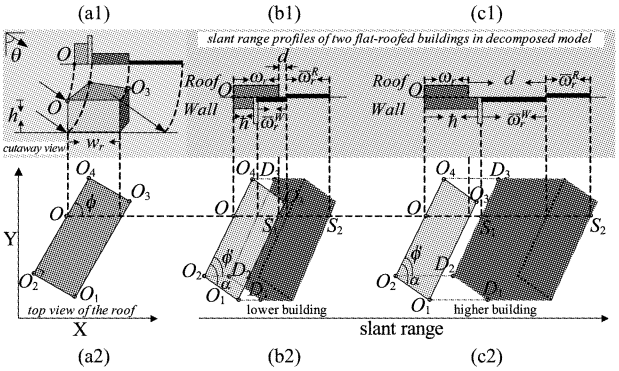

Fig. 1 (a1), (a2) are the cutaway view (up) and the top view (down), respectively, of flat-roofed building under incidence angle and aspect angle . (b1), (c1) are the illustration of the backscattering of two flat-roofed buildings in the range direction under the off-nadir angleusing decomposed model (in the blue block). (b2), (c2) are the detailed structures of the two flat-roofed buildings with different heights under aspect angle

图 1　平顶建筑的分解示意图

1) roof signal and shadow

$$\omega_r = w_r \sin\theta \quad , \quad (1)$$

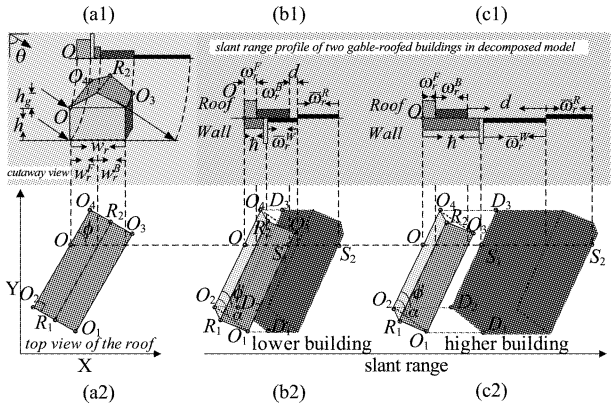

Fig. 2 (a1), (a2) are the cutaway view (up) and the top view (down), respectively, of gable-roofed building with incidence angle and aspect angle . (b1), (c1) are the illustration of the backscattering of right-angled buildings in the range direction under the off-nadir angleusing decomposed model (in the blue block). (b2), (c2) are the detailed structures of two gable-roofed buildings with different heights under aspect angle

图2 尖顶建筑的分解示意图

$$\omega_r^F = w_r^F \sin\theta - h_g \cos\theta \quad , \quad (2)$$

$$\omega_r^B = (w_r - w_r^F)\sin\theta + h_g\cos\theta \quad , \quad (3)$$

$$\bar{\omega}_r^R = w_r \sin\theta \quad , \quad (4)$$

where ω_r, ω_r^F and ω_r^B represent range dimensions of the whole roof reflection, sensor-near roof patch reflection and sensor-far roof patch reflection, respectively. $\bar{\omega}_r^R$ shows the range size of the shadow area caused by roof.

The interval distance between roof signal and roof shadow is related to the wall height and the irradiated width w_r by

$$d = \max\left(\frac{h}{\cos\theta} - w_r \sin\theta, 0\right) \quad , \quad (5)$$

and wall signal and shadow by

$$\hbar = h\cos\theta \quad , \quad (6)$$

$$\bar{\omega}_r^W = \frac{h\sin^2\theta}{\cos\theta} \quad , \quad (7)$$

where $\hbar$ and $\bar{\omega}_r^W$ indicates the range sizes of wall signal and wall shadow, respectively. Specially, the double-bounce reflections caused by the corner of the wall and ground appear as bright lines located at the far end of wall signal, which can be used for building detection or height retrieval[4].

1.2 Decomposed analysis of building appearance under non-orthogonal viewing direction

The aspect angle ϕ has strong impact on the appearance of buildings in SAR data, which always makes the interpretation and processing a tough task. However, in VHR SAR data, with more discernable structures (edges, roof patches), the influence of aspect angles could be modeled and exploited in feature recognition.

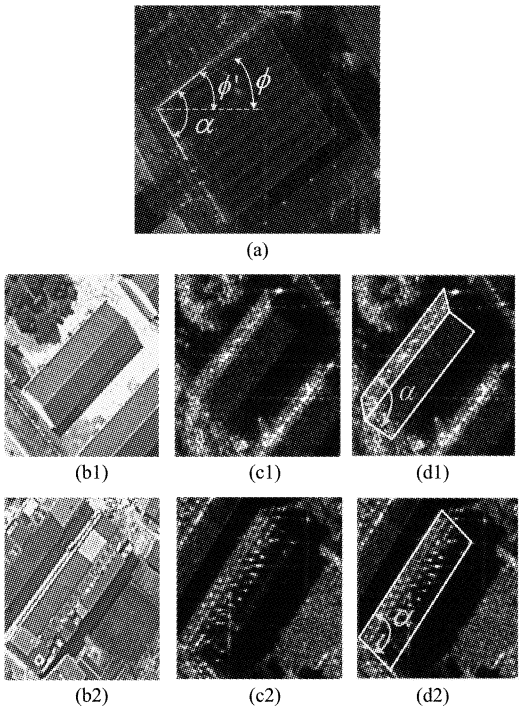

Fig. 3 (a) defines ϕ, α, ϕ' in VHR SAR image of a building, where the red dot line denotes the rectangular in scene space, the yellow line denotes outline of the projection angle. (b1)-(b2) show the google earth images of a flat-roofed building and a gable-roofed building. (c1)-(c2) are the appearance of a flat-roofed building and a gable-roofed building in airborne SAR image with resolutions 0.5 m and 0.25 m, respectively. (d1)-(d2) show the marked projective angle in airborne SAR images

图3 ϕ, α, ϕ'在SAR图像的示意;平顶尖顶房屋的示意图

Firstly, the projection of a right-angle pointing to the sensor in SAR image can be characterized by the following relations:

$$\tan\alpha = \frac{2\sin\theta}{(\sin^2\theta - k^2)\sin 2\phi} \quad , \quad (8)$$

$$k \cdot \tan\phi = \sin\theta \cdot \tan\phi' \quad , \quad (9)$$

where α is the projective angle of a flat right-angle in SAR image under incidence angle θ and aspect angle ϕ, ϕ' is the measured rotating angle from image (shown in Fig. 3(a)), is the ratio of the slant range resolution δ_{sr} and azimuth resolution δ_a ($k = \delta_{sr}/\delta_a$). α

is a judging index of the existence of a flat rectangle and can also be used in the extraction of the weak side of a flat rectangle.

In Figs. 1 (b2) and (c2), the appearances of two flat buildings with different heights are modeled under the same aspect angle ϕ. The quadrate roof in the image coordinates (y-r plane) appears as a parallelogram ($O_1O_2O_3O_4$) with internal angle equal to α. From the roof parallelogram, length l and width w can be calculated by the following relations:

$$w = w_r \sin\phi = \frac{\omega_r \sin\phi}{\sin\phi} \quad , \quad (10)$$

$$l = \sqrt{\left(\frac{1_r}{\sin\theta}\right)^2 + 1_a^2} \quad , \quad (11)$$

where ω_r corresponds to the measured width of $O_1O_2O_3O_4$ in range direction, 1_r, 1_a are the length of line O_4O_2 in the range and azimuth direction, respectively.

The echoes from the walls appear as two parallelograms $O_1O_2D_1D_2$ and $O_2O_4D_2D_3$. One pair of parallel edges of each wall parallelogram has the same slope as the roof edge (O_1O_2 or O_2O_4, respectively), while the other pair of edges are along the range direction. This structural information can be used to deduce the signal type, or used as prior knowledge to restrict the distribution of wall scattering during feature extraction. The height of the wall could be retrieved by the size of the edge which is along slant range direction using formula (6). The double-bounce lines D_1D_2 and D_2D_3 are strong indicators of the far-range edges of wall parallelograms.

The shadow area contains nearly all geometric information of a building. To understand the shadow shape, it is subdivided into roof shadow and wall shadow. The wall shadow is adjacent to the wall echo, and the roof shadow is next to the wall shadow. The dividing lines are shown with black dots. The wall shadow has the same structure as wall signal but different in size in range direction, while the roof shadow is the same as the roof signal. Based on decomposed analysis, the shadow shape is easily modeled under any aspect angle. Also, more useful information is available for the utilization, like, if the shadow is convex, which means the building is comparatively high, the height of the wall could be retrieved from the length of S1 S2 by Eqs. (4) and (7); if the shadow is concave, which means the building is low, the wall height should be calculated from the S1 S2 by Eqs. (4) and (5).

In Figs. 2 (b2) and (c2), the appearances of two gable-roofed buildings with different heights under aspect angle ϕ are illustrated. In comparison with flat buildings, the roof area of gable building is subdivided into two parallelograms with different intensity and shape, as shown in Figs. 3 (c1) ~ (c2), where the real magnitude images of a flat-roofed and a gable-roofed building are displayed (see more detail in Fig. 4). Still, the four roof corner points (O1, O2, O3, O4) form a parallelogram with internal angle equal to , the projection of a flat right angle under the same illumination condition calculated by Eq. (8). In the case that the intensity information is not sufficient to recognize the roof type, the measured internal angle of the roof parallelogram is compared with to identify the roof type. In Figs. 3 (d1) and (d2), internal angles of roof parallelograms of different roof types and their relation with α is displayed.

The roof height h_g can be retrieved by Eqs. (2) and (3), or from $\hbar_g$, the range distances between R1 and M1, as follow:

$$h_g = \frac{\hbar_g}{\cos\theta} \quad . \quad (12)$$

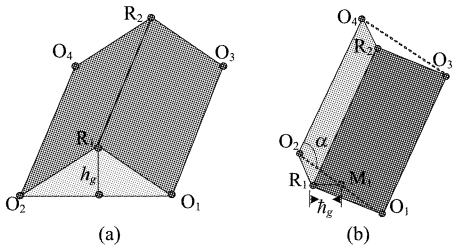

Fig. 4 (a) Model of gable roof with height h_g. (b) The appearance of gable roof in SAR image, $\hbar_g$ is the distance from R_1 to M_1 in slant range direction

图 4 尖顶建筑模型及在 SAR 图像上的投影示意图

2 Building detection and reconstruction from single VHR SAR image

To reconstruct a rectangular building, eight parameters are required, containing the center position (x_0, y_0), the aspect angle ϕ, the width, length and

height (w,l,h), the roof height h_g and the width of the sensor near roof patch w^F. Based on the aforementioned analysis of building signature in VHR SAR data, we model the appearance of rectangular building as a regular combination of feature parallelograms corresponding to the scattering effects from roof and wall, respectively.

2.1 Match-based feature extraction from VHR SAR image

Benefited from the prior knowledge about the shape of image features, the extraction can be performed as a match process. A parallelogram hypothesis is generated by its initial parameters and is compared to the actual scene. Then, the unknown parameters are continuously adjusted until an optimal match is achieved. The final parallelogram is corresponding to the hypothesis which matches best with actual data. The optimal parameter $\hat{X}$ of parallelogram is given by:

$$\hat{X} = \arg\max_X F(P(X)) \quad , \quad (13)$$

where X is the parameter of the hypothesized parallelogram P, F denotes the matching function defined as follows:

$$F(P) = \gamma_e \frac{\sum_{(m,n)\in P} f(m,n)}{N(P)} + \gamma_r \left(\sum_{i=1}^{4} |\bar{u}_{ip} - \bar{u}_p|^2 - \sigma_P^2 \right) \quad , \quad (14)$$

where $N(P)$ is the number of the boundary of P, f is the ROA edge map [7] of the actual image, $\bar{u}_p$ and σ_p^2 denote the mean and deviation of the region inside P, $\bar{u}_{ip}$ is the mean of one of the four outside stripes round region P in the magnitude image. The first term of Eq. (14) measures the similarity between the predicated parallelogram contour and the detected edge. The second term measures inner homogeneity of region inside P and the heterogeneity of regions inside and outside P. γ_e and γ_r are coefficients for the two terms.

One parallelogram has six independent parameters at most. To retrieve all eight geometrical parameters of one building, more feature parallelograms with eight independent parameters are needed. All feature parallelograms are extracted via the match procedure. Features of different types have different characteristics as well as the degrees of influence from edge or region. So the values of γ_e and γ_r are selected empirically according to the feature type to emphasize the influence of edge or region.

2.2 Knowledge-based detection and reconstruction process

In VHR SAR images, the roof and edge signal with bright intensity are well detectable and are less interfered by nearby objects. Thus, in our approach, the bright roof parallelogram is detected and extracted first. The rest features are extracted in order according to configuration of the building area.

The algorithm is divided into two main steps as follows:

1) Detection step: First, the preprocessing is performed for anisotropic diffusion [8] to the original SAR image (Fig. 5a) to smooth regions while enhance the contrast at sharp intensity gradients. Then, bright regions with regular shape and long edge lines are segmented from the preprocessed image (Fig. 5b) by threshold-based segmentation. Areas around the bright regions (Fig. 5c) are supposed to be potential building areas.

2) Reconstruction step: The ratio edge detector [7] and ridge filter [2] are applied to each potential building area to get the edge map (Fig. 5d). The longest and most continuum line which is supposed to be one of the long edges of the roof parallelogram is extracted by Hough transform (Fig. 5e). From the edge line, two parameters, the actual aspect angle ϕ and the supposed projective angle α of a flat right angle under ϕ are calculated by formulas (8) and (9). Also, with one edge line fixed, a series of parallelogram hypothesis are generated by changing the center position of the parallelogram. The final roof parallelogram is obtained by maximizing the match function (14). Once the roof parallelogram is fixed (Fig. 5f), the roof type is determined by comparing its measured internal angle with. If the roof is flat, the roof height hg is equal to 0. If the roof is gable, another roof parallelogram will be extracted next. Based on the spatial relation with the first roof parallelogram, the second one has only one unknown parameter to be estimated following the matching procedure (Fig. 5g). Building height is linked with the range size of shadow or wall signal in formulas (4) ~ (7). It

can be retrieved by either of the features. In order to obtain a more robust result, height retrieval is done by extracting all possible features. For shadow feature, based on the roof parallelograms, the basic shape and distribution of the shadow area is fixed. Thus, the dark parallelogram between two middle roof corner points (Fig. 5h) is extracted instead of the whole shadow area using the matching procedure. For wall parallelogram extraction, double-bounce lines, if existed, are utilized in locating the far-range edge of the wall parallelogram. The final height is dependent on the weighted mean value of all available results.

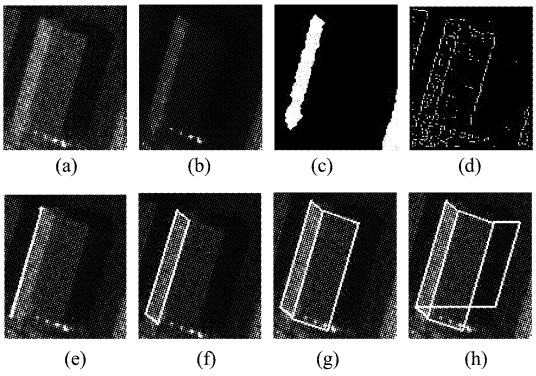

Fig. 5　Steps for extraction of image characters of a building. (a) An original VHR SAR image of a gable-roofed building. (b) The result of preprocess. (c) The bright region. (d) ROA edge map of the bright region. (e) The line detection. (f) The first parallelogram. (g) The second parallelogram. (h) The shadow detection
图 5　分步提取建筑物图像特征

We have to mention that not rectangular buildings of any size could be retrieved by this method. The sizes of the buildings which could be detected and reconstructed are determined by the image resolution. The higher the resolution is, the finer the building structure could be discernable, and the smaller the buildings could be extracted.

3　Experiments

To demonstrate the performance of the proposed approach, we applied it to airborne VHR SAR image acquired during a flight campaign in the area of BaYi town, Sichuan province, China, in 2011. The test image (Fig. 6a) has been obtained with radar working in X band, an incidence angle of $45^\circ \sim 50^\circ$ and geometric resolutions of 0.25m × 0.25m (azimuthslant range). In Fig. 6(b), the photograph of the same site is used as references.

There are eight gable-roofed buildings (labeled in Fig. 6) with different aspect angles detected by our approach in this area. The detection results are shown in Fig. 6(c), the bright roof areas which are supposed to be the indicators of buildings are detected and labeled on the preprocessed images. The feature extraction results are shown in Fig. 6 (d). All the roof parallelograms are marked by yellow lines, and the extracted shadow areas which contain the height information are marked with white lines. Specially, for buildings 5, 6, 7, there are no shadows available, and the double-bounce lines are discernable as there is no occlusion in front. Thus the building height is retrieve through the distance of double-bounce lines and roof edges. Also, for buildings 1, 2, the shadow area is partly occluded by the reflection of building behind. The size of shadow parallelogram needs to be extracted shrink to fit the situation. The ground truth and the reconstruction results are listed in Table I. In comparison with the ground truth data, the reconstructed results of buildings 1 ~ 4 show an underestimation of the building length due to the interference from nearby objects,

Table 1　Building reconstruction results and ground truth data
表 1　建筑物重建结果及实际数据对比

index	length	width	wall height	roof height	l(m)	w(m)	h(m)	h_g(m)	ϕ	$\Delta(h_g+h)$
1	19 m	14 m	5.2 m	2.8 m	18.10	14.59	5.06	3.11	70.0°	0.17 m
2	26 m	14 m	5.2 m	2.8 m	24.16	14.29	5.30	2.42	70.3°	-0.28 m
3	28.5 m	14 m	3.6 m	3.4 m	24.28	13.75	3.54	3.30	69.5°	-0.16 m
4	30 m	11.5 m	3.5 m	3.4 m	29.08	12.85	3.37	3.60	71.0°	-0.07 m
5	30 m	11.5 m	3.5 m	3.4 m	26.98	14.21	4.28	3.57	70.9°	0.85 m
6	19 m	14 m	5.2 m	2.8 m	18.23	13.53	5.45	2.43	71.2°	-0.12 m
7	16.5 m	8 m	3.3 m	2.2 m	16.54	7.69	3.11	2.35	-14.9°	-0.04 m
8	42 m	7.9 m	3.2 m	2.0 m	40.95	7.27	3.37	2.36	-18.5°	0.53 m

while the retrieval of other parameters shows good results. The reconstructions of buildings 5 and 6 have the maximum estimated errors of height, since they are surrounded by tall trees which prevent the detection of features containing height information. Building 7 which is less affected by its surroundings in range direction has the lowest difference between estimated dimensions and the ground truth. Building 8 composed by two adjacent buildings is detected as a single one, but the reconstruction results are quite satisfying. To further evaluate the usability of our method, we simulated buildings 3 and 7 based on the reconstructed 3-D models using the SAR image simulator in [9]. The real buildings, 3-D models and the simulated results are shown in Fig. 7. The real and simulated images show a good match in the geometrical distributions of main scattering effects.

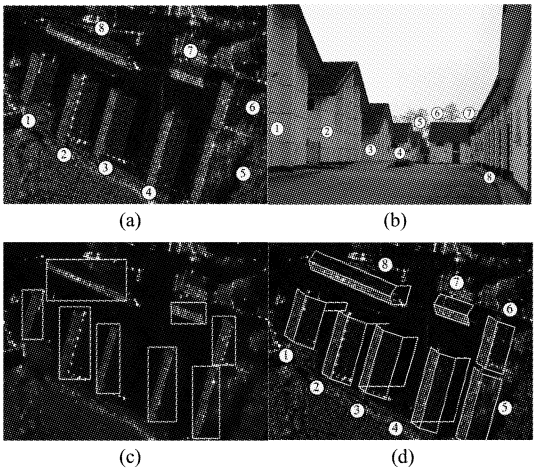

Fig. 6 (a) Airborne VHR SAR image of area in BaYi town (2011). (b) Photo of the tested area (2012). (c) The building detection results on the preprocessed image. (d) The feature extraction results, the roof parallelogram are marked by yellow lines, the double-bounce lines are marked by red lines, and the white lines represent the extracted shadow areas which contains the height information

图6 (a)八一镇的机载高分辨率SAR图像和提取结果

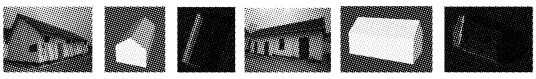

Fig. 7 (a1) ~ (a2) Photos of buildings 3 and 7, (b1) ~ (b2) Reconstructed 3D models. (c1) ~ (c2) Simulated SAR images

图7 建筑物3和建筑物7的图片,模型,仿真图像

4 Conclusion

In this paper, we proposed a decomposed model to analyze the rectangular building signature in of VHR SAR data. The generalized expressions which link the building dimensions to image features are free of ambiguity problem and detailed structural information of image features of buildings is extracted. Based on the recognized effects, a new detection and reconstruction approach was proposed which contain the match-based feature extraction and the knowledge-based reconstruction process. The reconstruction results well demonstrate the validity of the proposed method. In future work, multi-bounce scattering effects and the influence of adjacent objects will be analyzed. The detection and reconstruction algorithm will be further improved to be applied in more complex scenes.

REFERENCES

[1] Thiele A, Cadario E, Schulz K, *et al*. Analysis of gable-roofed building signature in multiaspect InSAR data [J]. *IEEE Geoscience and Remote Sensing Papers*, 2010,7(1): 83 - 87.

[2] Xu F, Jin YQ. Automatic Reconstruction of Building Objects From Multiaspect Meter-Resolution SAR Images [J]. *IEEE Transactions on Geoscience and Remote Sensing*, 2007 (45) 7: 2336 - 2353.

[3] Wegner J D, Ziehn J R, Soergel U. Building detection and height estimation from high-resolution InSAR and optical data [C]. *in International Geoscience and Remote Sensing Symposium (IGARSS)*. U. S. A, 2010: 1928 - 1931.

[4] Guida R Iodice A, Riccio D. Height retrieval of isolated buildings from single high-resolution SAR images [J]. *IEEE Trans. Geosci. Remote Sensing*. 2010: 2967 - 2979.

[5] Brunner D, Lemoine G, Bruzzone L, *et al*. Building height retrieval from VHR SAR imagery based on an iterative simulation and matching technique [J]. *IEEE Trans. Geosci. Remote Sensing*. 2010(48): 1487 - 1504.

[6] Soergel U, Thoenessen U, Brenner A, *et al*. High resolution SAR data: new opportunities and challenges for the analysis of urban areas[C]. *IEE Proceedings - Radar, Sonar, Navigation*, 2006.

[7] Touzi R, Lopes A, Bousquet P. A Statistical and Geometrical Edge Detector for SAR Images [J]. *IEEE Transactions on Geoscience and Remote Sensing*, 1988 (26) 6: 764 - 773.

[8] Perona P, Malik J. Scale-space and edge detection using anisotropic diffusion [J]. *IEEE Trans. Pattern Anal. Machine Intell*, 1990 (12): 629 - 639.

[9] Tang K, Sun X, Sun H, *et al*. A Geometrical-based Simulator for Target Recognition in High Resolution SAR Images [J]. *IEEE Geosciece and Remote Sensing Papers*. 2012 (9) 5:958 - 962.